

# Single-Tone Frequency Estimation by Weighted Least-Squares Interpolation of Fourier Coefficients

Michele Morelli, Marco Moretti and A. A. D'Amico

**Abstract**—Frequency estimation of a single complex exponential signal embedded in additive white Gaussian noise is a major topic of research in many engineering areas. This work presents further investigations on this problem with regards to the fine estimation task, which is accomplished through a suitable interpolation of the discrete Fourier transform (DFT) coefficients of the observation data. The focus is on fast real-time applications, where iterative estimation methods can hardly be applied due to their latency and complexity.

After deriving the analytical expression of the Cramér-Rao bound (CRB) for general values of the system parameters, we present a new DFT interpolation scheme based on the weighted least-squares (WLS) rule, where the optimum weights are precomputed through a numerical search and stored in the receiver. In contrast to many existing alternatives, the proposed method can employ an arbitrary number of DFT samples so as to achieve a good trade-off between system performance and complexity. Simulation results and theoretical analysis indicate that, at sufficiently high signal-to-noise ratios, the estimation accuracy is close to the relevant CRB at any value of the frequency error. This provides some advantage with respect to non-iterative competing schemes, without incurring any penalty in processing requirement.

**Index Terms**—Frequency estimation, least-squares methods, DFT interpolation.

## I. INTRODUCTION

Frequency estimation of a complex sinusoidal signal embedded in white Gaussian noise plays a major role in many technological areas, including radar applications [1], power grid systems [2] and biomedical signal processing. In wireless communication systems, fast and accurate frequency recovery is a fundamental task for carrier synchronization and for compensating large Doppler shifts arising in transmissions with high-speed trains, flying vehicles and low earth orbit satellites. The maximum likelihood (ML) solution to this problem was derived in [3] and involves maximizing the periodogram of the observed data with respect to the unknown frequency. Since no closed-form expression is available to locate the maximum of the periodogram, a suboptimal approach is typically adopted which operates in two steps: a coarse search followed by a fine-tuning stage. In the first step, DFT analysis is used to evaluate a set of uniformly spaced samples of the signal spectrum, and the DFT coefficient with the highest magnitude is selected. The subsequent fine-tuning step tries to refine the coarse frequency estimate through a dichotomous search or a suitable interpolation of the DFT samples. A common feature of any frequency estimator (operating either in the time or in

the frequency domain) is the presence of large errors, called outliers, that may occasionally occur at low signal-to-noise ratios (SNRs).

Single-tone frequency estimation through DFT interpolation is a well investigated subject and many solutions are currently available. In general, they can be divided into two categories: direct methods [4]-[17] and iterative schemes [18]-[25]. The former employ a few DFT coefficients obtained from the initial coarse search and provide the final frequency estimate with negligible additional cost. For this reason, they are particularly attractive for fast real-time applications, including voice communications, carrier synchronization and tracking of moving radar targets. In general, their accuracy is non-uniform over the entire search range and, quite surprisingly, the worst case occurs when the signal frequency corresponds to one of the DFT bins. Iterative methods operate in a recursive fashion, where the refined estimate of an earlier iteration is treated as the coarse estimate of the next until convergence. At each new iteration, two DFT samples are typically re-computed from the received discrete-time observations, with the DFT frequencies being symmetrically placed around the frequency estimate obtained from the previous iteration. This operation requires off-line signal processing, which makes such schemes unsuitable for real-time applications. Compared to direct methods, they achieve improved uniform performance at the expense of an increased computational load.

Among the direct methods, it is worth mentioning the parabolic interpolation of the periodogram [4] and the interpolator presented in [5], which was later extended to multi-sinusoidal signals in [6]. These schemes only exploit the amplitude of the DFT samples and exhibit poor performance. The phase component was considered in [7] and [8], where the maximum DFT coefficient and its two adjacent neighbours are used for fine frequency tuning. Macleod in [9] modified the interpolator of [8] and also proposed a five-sample interpolator. A scheme that can utilize an arbitrary number of DFT coefficients is presented in [10] to further improve the system performance. The authors of [11] suggest a modification of the parabolic interpolator based on empirical considerations. Its analytical derivation, together with an improved bias-corrected version, is presented by Candan in [12] and [13]. Further results on the bias correction problem can be found in [14], where a new set of unbiased estimators is derived by looking for the analytical relationship between the frequency error and the DFT samples. Alternative methods presented in [15], [16] and [17] employ two DFT coefficients placed midway between the DFT peak and its neighbours. This results into a finer frequency grid, which improves the system performance with a remarkable penalty in terms of processing requirement.

Michele Morelli (michele.morelli@unipi.it), Marco Moretti (marco.moretti@unipi.it) and Antonio A. D'Amico (antonio.damico@unipi.it) are with the Dipartimento di Ingegneria dell'Informazione, University of Pisa, Italy.

The iterative approach can employ a dichotomous search [18], the Newton algorithm [19] or other specific methods to retrieve the fractional frequency error. In [20], Aboutanian and Mulgrew presented two asymptotically unbiased iterative schemes with a uniform variance that is only 1.0147 times the classical Cramer-Rao bound (CCRB) computed in [3]. At each new iteration, two DFT coefficients are evaluated by applying a shift of  $\pm 0.5\Delta f$  to the frequency estimate obtained from the previous stage, where  $\Delta f$  is the distance between adjacent DFT bins. By resorting to the fixed-point theorem, it is shown that such schemes achieve convergence after two iterations, thereby requiring the calculation of four additional DFT coefficients placed at midpoint frequencies. Methods to save the calculation of two auxiliary DFT coefficients at the first iteration, which can still achieve the same accuracy of [20], are presented in [21]-[23]. More recently, it was reported in [24] that using fractional shifts other than  $\pm 0.5\Delta f$  may lead to improved system performance. Following this idea, the authors of [25] derived a novel scheme that needs computation of four auxiliary spectral lines and asymptotically attains the CCRB after two iterations.

In this paper we further investigate the DFT interpolation task for fast frequency estimation in real-time applications. In doing so, we concentrate on the class of direct interpolation schemes, which provide the final estimate without computing any other DFT coefficient in addition to those already available from the coarse search stage. One fundamental question is related to the best possible performance achievable by a frequency estimator belonging to this class. The answer is provided by the relevant CRB when only a reduced set of DFT coefficients is employed as observation variables. In that connection, a first contribution of our work is the analytical derivation of such a bound, which is different from the CCRB presented in [3]. In particular, the latter cannot be applied to direct interpolation methods as it was obtained assuming that all the DFT samples are involved in the frequency recovery task. Although plots of the novel CRB as a function of the residual frequency error have been previously shown in [9] in a few specific scenarios, no analytical formulation is available in the literature for the general case. The novel expression of the CRB is exact and holds true with any set of system parameters, including the residual frequency error, the number of selected DFT coefficients and the length of the data record. In this regard, it generalizes some known asymptotic results presented in [8] and [20], which are only suitable for large data sets. After a thorough review of the existing literature, we noted that available direct DFT interpolators are not able to achieve the new CRB for any value of the frequency error. This suggests that some improvement of the system performance is still possible, thereby motivating the search for some novel scheme that can attain the bound. Regarding this issue, the second contribution of our study is the derivation of a new non-iterative DFT interpolation algorithm based on the weighted least square (WLS) optimization criterion. In contrast to most existing methods which can only interpolate among two or three samples of the signal spectrum, the proposed scheme can utilize an arbitrary number of DFT bins. Theoretical analysis conducted in the high SNR regime is

used for the design of the optimal weighting coefficients. For this purpose, we use an exhaustive grid-search which does not affect the complexity of the proposed scheme, since the weights can be computed in advance and stored in the receiver. The resulting estimator can be used for real-time frequency recovery and exhibits the best accuracy within the class of direct interpolation methods. Compared to iterative schemes, it allows substantial computational saving while achieving comparable performance through a judicious choice of the number of interpolated DFT coefficients.

The remainder of the paper is organized as follows. The next section provides the signal model and introduces basic notations. In Sect. III, we present the analytical expression of the CRB when a restricted set of DFT samples is observed for frequency recovery. The new interpolator is derived in Sect. IV, where a criterion for the design of the optimum weighting coefficients is also formulated. Simulation results are illustrated in Sect. V, while some conclusions are drawn in Sect. VI.

## II. SYSTEM MODEL

We consider a single discrete-time complex exponential signal embedded in white Gaussian noise (WGN). The data samples are given by

$$x(n) = Ae^{j(n\omega+\varphi)} + w(n) \quad n = 0, 1, \dots, N-1 \quad (1)$$

where  $N$  is the observation length, while  $(A, \omega, \varphi)$  are unknown parameters which specify the amplitude, angular frequency and initial phase of the signal component. The noise terms  $\{w(n)\}$  are modeled as circularly-symmetric and statistically independent Gaussian random variables with zero mean and variance  $\sigma^2 = E\{|w(n)|^2\}$ . Accordingly, the SNR is defined as  $A^2/\sigma^2$ .

Our goal is the estimation of the angular frequency  $\omega \in [-\pi, \pi)$  in the presence of the unknown quantities  $(A, \varphi)$ , which are treated as *nuisance* parameters. This problem has application in many technological areas and represents a classical topic in signal processing. In wireless communication systems, it mainly arises in the context of carrier synchronization for coherent demodulation of the received waveform. Consider, for example, a pilot-assisted digital transmission, where a sequence of known symbols with unit amplitude  $\{d_n\}$  is periodically inserted in the transmitted data stream. After passing through the matched filter, the incoming signal is sampled at proper timing instants, yielding

$$y(n) = Ad_n e^{j(n\omega+\varphi)} + \eta(n) \quad n = 0, 1, \dots, N-1 \quad (2)$$

where  $\{\eta(n)\}$  is a white Gaussian process with variance  $\sigma^2$ . Multiplying  $y(n)$  by  $d_n^*$  and observing that  $\{d_n^* \eta(n)\}$  is statistically equivalent to  $\{w(n)\}$ , we eventually get the observation variables specified in (1).

The estimation of  $\omega$  from the time series  $\{x(n)\}$  was originally studied by Rife and Boorstyn in [3], where it is shown that the ML solution is the value  $\hat{\omega}_{ML}$  maximizing the periodogram

$$\Gamma(\tilde{\omega}) = \frac{1}{N} \left| \sum_{n=0}^{N-1} x(n) e^{-jn\tilde{\omega}} \right|^2 \quad (3)$$

with respect to the continuous variable  $\tilde{\omega} \in [-\pi, \pi)$ . The ML estimator is asymptotically unbiased and attains the CCRB, which is expressed by

$$\text{CCRB} = \frac{6(\text{SNR})^{-1}}{N(N^2 - 1)}. \quad (4)$$

Unfortunately, locating the maximum of the periodogram in (3) is computationally demanding as it requires a grid search over the set spanned by  $\tilde{\omega}$ . A popular reduced-complexity approach relies on the following expression of the angular frequency  $\omega$

$$\omega = \frac{2\pi(k_p + \varepsilon)}{N} \quad (5)$$

where  $k_p$  is an integer-valued parameter referred to as integer frequency offset (IFO) and  $\varepsilon \in [-0.5, 0.5)$  is the residual fractional frequency offset (FFO). The maximization process is thus split into two successive stages. The first step (coarse search) employs the  $N$ -point DFT of  $\{x(n)\}$ , i.e.,

$$X(k) = \sum_{n=0}^{N-1} x(n)e^{-j2\pi nk/N} \quad k = 0, 1, \dots, N-1 \quad (6)$$

and provides the IFO estimate  $\hat{k}_p$  as the location where  $|X(k)|$  achieves its global maximum. The second step (fine search) makes an interpolation between the peak DFT sample  $X(\hat{k}_p)$  and a specified number of neighbours to get the FFO estimate  $\hat{\varepsilon}$ . At low SNR values, the maximum of  $|X(k)|$  may occasionally occur far from  $k_p$  as a consequence of noise-induced distortions. When this happens, the estimator makes large errors, known as *outliers*, which deteriorate the system performance. The SNR value below which the outliers start to occur is called the threshold of the estimator. Such a peculiar phenomenon is typical of any nonlinear estimation problem and also appears in the true ML scheme that looks for the maximum of  $\Gamma(\tilde{\omega})$ . In the context of DFT interpolation, there is a common belief that the SNR threshold can be reduced by adopting the zero-padding strategy so as to obtain a finer frequency resolution during the coarse search. As shown in [3], however, zero-padding has only a marginal impact on the insurgence of outliers and, for this reason, it is not considered in the foregoing discussion. The only viable way to reduce the SNR threshold is to enlarge the observation set using higher values of  $N$ . In practice,  $N$  must be properly designed so that the estimator can operate well above its SNR threshold.

Our work is focused on the DFT interpolation stage, assuming that the coarse search has been successfully completed, which amounts to putting  $\hat{k}_p = k_p$ . Since we are interested in fast frequency recovery for real-time applications, we only concentrate on the *direct* approach to DFT interpolation, so as to avoid the need for computing any auxiliary DFT coefficient in addition to those evaluated during the initial coarse search. Observing that the accuracy of direct methods cannot attain the CCRB shown in (4) as a consequence of the reduced number of observations, it is important to firstly establish the best accuracy that can be achieved by any direct DFT interpolator. This may reveal useful to check whether some improvement of the system performance is possible or not with respect to existing schemes. For this purpose, we start

our study by deriving the CRB for the estimation of  $\omega$  when a small set of contiguous DFT samples, selected from  $\{X(k); k = 0, 1, \dots, N-1\}$  and placed around  $X(k_p)$ , are the only available observation variables. This bound has been plotted in [9] as a function of  $\varepsilon$ , but without providing its analytical formulation. Asymptotic expressions for large block lengths can be found in [8] in a few specific cases. To the best of our knowledge, no analytical expression of this CRB is available for the general case. Next, we show how the selected DFT samples can be exploited to get a frequency estimator that performs close to the relevant CRB for any value of the FFO.

### III. CRAMÉR-RAO BOUND FOR DFT INTERPOLATORS

We assume ideal knowledge of the IFO  $k_p$  and investigate the ultimate accuracy achievable in the estimation of  $\omega$  when a specified number  $L$  of contiguous DFT samples are used as signal measurements. The latter are placed around the DFT peak  $X(k_p)$  and are collected into a vector  $\mathbf{X}_L = \{X(k_p + k); -L_1 \leq k \leq L_2\}$ , where  $L_1$  and  $L_2$  are non-negative integer parameters. Intuitively, the best performance is attained when the  $L$  DFT bins used for interpolation are those closest to the signal frequency  $\omega$ . This implies that  $L_1$  is chosen according to the rule

$$L_1 = \begin{cases} (L-1)/2 & \text{if } L \text{ odd} \\ L/2 - 1 & \text{if } L \text{ even and } \varepsilon \geq 0 \\ L/2 & \text{if } L \text{ even and } \varepsilon < 0 \end{cases} \quad (7)$$

and  $L_2$  is consequently set to  $L_2 = L - L_1 - 1$ . It is worth observing that, when  $L$  is even, the optimal selection of the DFT samples specified in (7) requires prior knowledge of the polarity of  $\varepsilon$ .

The entries of  $\mathbf{X}_L$  are found by substituting (1) into (6). This yields

$$X(k_p + k) = S_L(k) + W_L(k) \quad -L_1 \leq k \leq L_2 \quad (8)$$

where  $\{W_L(k)\}$  are circularly-symmetric and statistically independent Gaussian random variables with zero mean and variance  $\sigma_W^2 = N\sigma^2$ , while  $S_L(k)$  is expressed by

$$S_L(k) = (C_R + jC_I) \sum_{n=0}^{N-1} e^{jn\omega} e^{-j2\pi n(k+k_p)/N} \quad (9)$$

with  $C_R$  and  $C_I$  being the real and imaginary parts of  $Ae^{j\varphi}$ , respectively. Our goal is to find the CRB for the estimation of  $\omega$  based on the observation vector  $\mathbf{X}_L$  and in the presence of the nuisance parameters  $\{C_R, C_I\}$ . The following theorem summarizes the main result of this section.

*Theorem 1:* The CRB for  $\omega$  based on  $\mathbf{X}_L$  is

$$\text{CRB}(L, \varepsilon) = \frac{(\text{SNR})^{-1}}{2N} \cdot \frac{\|\boldsymbol{\alpha}\|^2}{\|\boldsymbol{\alpha}\|^2 \|\boldsymbol{\beta}\|^2 - |\boldsymbol{\beta}^H \boldsymbol{\alpha}|^2} \quad (10)$$

where  $\boldsymbol{\alpha} = \{\alpha(k); -L_1 \leq k \leq L_2\}$  and  $\boldsymbol{\beta} = \{\beta(k); -L_1 \leq k \leq L_2\}$  are  $L$ -dimensional vectors whose entries are reported in (46) and (47).

*Proof:* see Appendix A.

In (10), the notation  $\text{CRB}(L, \varepsilon)$  explicitly indicates the dependence of the CRB on parameters  $L$  and  $\varepsilon$ , while the

dependence on  $N$  is omitted for notational simplicity. The entries of  $\alpha$  and  $\beta$  depend on the FFO  $\varepsilon$  and can also be expressed in a more compact form as

$$\alpha(k) = \frac{1 - e^{j2\pi\varepsilon}}{N[1 - e^{-j2\pi(k-\varepsilon)/N}]} \quad (11)$$

and

$$\beta(k) = \frac{(N-1)e^{j2\pi[(N+1)\varepsilon-k]/N} - Ne^{j2\pi\varepsilon} + e^{-j2\pi(k-\varepsilon)/N}}{N[1 - e^{-j2\pi(k-\varepsilon)/N}]^2}. \quad (12)$$

It is worth noting that, in general,  $\text{CRB}(L, \varepsilon)$  is greater than the CCRB shown in (4) as a consequence of the reduced number of observation measurements. Clearly, the two bounds coincide when  $L = N$ . A simplified expression of  $\text{CRB}(L, \varepsilon)$  is possible when  $\varepsilon = 0$ , as specified in the following corollary.

*Corollary:* For  $\varepsilon = 0$ , the bound (10) takes the form

$$\text{CRB}(L, \varepsilon = 0) = \frac{2(\text{SNR})^{-1}}{N \sum_{k \in \mathcal{A}} \frac{1}{\sin^2(\pi k/N)}} \quad (13)$$

where  $\mathcal{A}$  collects all integers  $k$  such that  $-L_1 \leq k \leq L_2$ , with  $k \neq 0$ .

*Proof:* see Appendix A.

For any value of  $L$ , the right-hand-side of (13) achieves a minimum when  $L_1$  is chosen according to (7). This corroborates the idea that the rule expressed in (7) represents the optimal selection strategy of the DFT coefficients used for interpolation. At this stage, it is interesting to assess the loss incurred in the estimation of  $\omega$  when  $\mathbf{X}_L$  is taken as the observation vector instead of the entire set of  $N$  DFT coefficients. The loss can be quantified through the following *normalized CRB*

$$\text{NCRB}(L, \varepsilon) = \frac{\text{CRB}(L, \varepsilon)}{\text{CCRB}} \quad (14)$$

which is expressed by

$$\text{NCRB}(L, \varepsilon) = \frac{N^2 - 1}{12} \cdot \frac{\|\alpha\|^2}{\|\alpha\|^2 \|\beta\|^2 - |\beta^H \alpha|^2}. \quad (15)$$

Fig. 1 illustrates  $\text{NCRB}(L, \varepsilon)$  as a function of  $L$  for three different FFO values and  $N = 64$ . As is seen, the penalty incurred from using a reduced set of DFT samples for FFO recovery monotonically decreases with  $L$  and is rather small when  $L \geq 3$ . For  $\varepsilon = 0.5$ , the penalty virtually disappears even with  $L = 2$ , despite the fact that this situation causes maximum leakage in the DFT spectrum.

Similar conclusions can be drawn by inspection of Fig. 2, where  $\text{NCRB}(L, \varepsilon)$  is shown versus  $\varepsilon \in [0, 0.5]$  with  $L$  as a parameter and  $N = 64$ . For each value of  $L$ , the loss with respect to the full ML estimator is maximum when  $\varepsilon = 0$  and monotonically decreases with  $\varepsilon$ . For  $\varepsilon > 0.3$ , such a loss depends weakly on  $L$  and becomes vanishingly small as  $\varepsilon$  approaches 0.5. These plots are also reported in [9] for the two cases  $L = 3$  and  $L = 5$ , but without providing their mathematical formulation. Bearing in mind (13), for  $\varepsilon = 0$  we have

$$\text{NCRB}(L, \varepsilon = 0) = \frac{N^2 - 1}{3 \sum_{k \in \mathcal{A}} \frac{1}{\sin^2(\pi k/N)}} \quad (16)$$

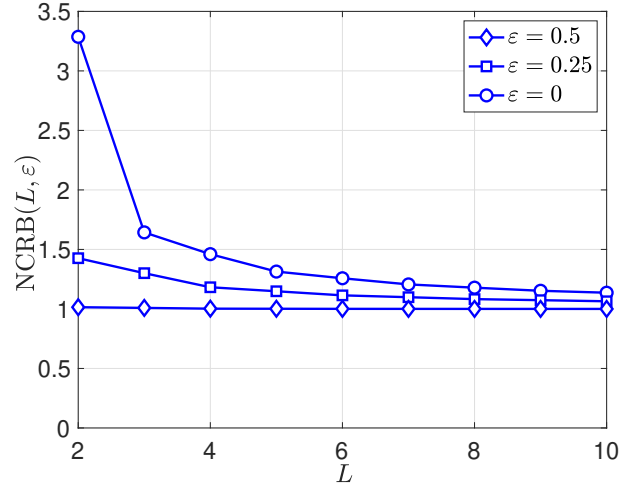


Fig. 1.  $\text{NCRB}(L, \varepsilon)$  as a function of  $L$  for three different FFO values and  $N = 64$ .

which demonstrates how the loss can be reduced by increasing  $L$ . It is worth mentioning that the analytical expression (16) is not available in the literature and can be applied with any value of  $L$  and  $N$ . In this sense, it generalizes some known results obtained with a few specific values of  $L$  and assuming large data blocks. For example, letting  $L = 2$  and  $L = 3$  in (16) yields

$$\text{NCRB}(L = 2, \varepsilon = 0) = \frac{N^2 - 1}{3} \sin^2\left(\frac{\pi}{N}\right) \quad (17)$$

$$\text{NCRB}(L = 3, \varepsilon = 0) = \frac{N^2 - 1}{6} \sin^2\left(\frac{\pi}{N}\right) \quad (18)$$

which, for large data sets, approach the asymptotic values  $\pi^2/3$  and  $\pi^2/6$  reported in [8]. Furthermore, putting  $\varepsilon = 0.5$  and  $L = 2$  into (15), after some manipulations we get

$$\text{NCRB}(L = 2, \varepsilon = 0.5) = \frac{N^2(N^2 - 1) \sin^4\left(\frac{\pi}{2N}\right)}{6 \cos^2\left(\frac{\pi}{2N}\right)} \quad (19)$$

which asymptotically attains the value  $\pi^4/96$  cited in [8] and [20].

#### IV. FREQUENCY ESTIMATION THROUGH WEIGHTED LEAST-SQUARES

Previous methods for frequency recovery through DFT interpolation are mostly based on suboptimal heuristic reasoning and do not obey to any specific optimality criterion. Some of them employ suitable approximations of the non linear relationship between the FFO and the DFT coefficients, which result into an estimation bias. Computer simulations presented later indicate that none of the existing direct DFT interpolators can attain the CRB given in (10). This prompted us to investigate whether some alternative scheme, which is optimal in some sense, can be found to improve the performance of existing methods. The result of our study is a novel fast frequency recovery scheme that belongs to the class of direct DFT interpolators. As shown later, its accuracy is close to the relevant CRB for any value of  $\varepsilon$ .

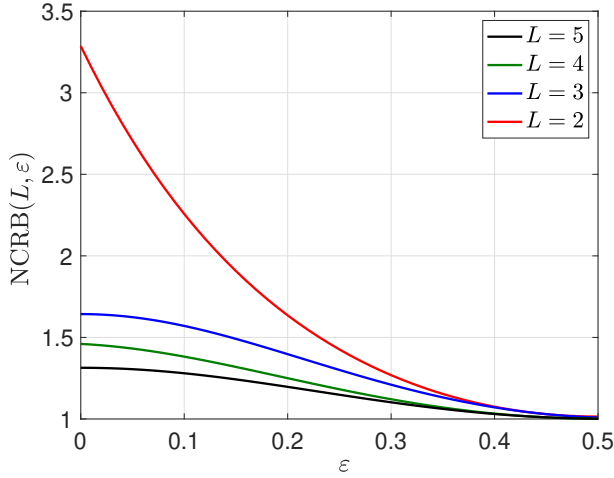


Fig. 2.  $\text{NCRB}(L, \varepsilon)$  vs.  $\varepsilon \in [0, 0.5]$  with  $L$  as a parameter and  $N = 64$ .

Furthermore, it can interpolate an arbitrary number of DFT samples, thereby allowing to achieve the desired trade-off between complexity and estimation accuracy. In particular, it can approach the performance of iterative DFT interpolators, but with a remarkable reduction of the processing load and latency.

#### A. Problem formulation

We still assume that the IFO has been correctly estimated during the coarse search and the DFT coefficients selected for fine frequency recovery are collected into the observation vector  $\mathbf{X}_L$ . Its entries are denoted by  $X_L(k) = X(k_p + k)$  for  $-L_1 \leq k \leq L_2$ , where  $L_1$  is chosen as specified in (7) and  $L_2 = L - L_1 - 1$ . The mathematical model of  $X_L(k)$  is given in (8) and (9). In particular, after evaluating the summation in the right-hand-side of (9), it can be reformulated as

$$X_L(k) = \frac{b}{1 - ae^{-j2\pi(k+k_p)/N}} + W_L(k) \quad (20)$$

where  $W_L(k)$  is the noise term and we have used the notation  $b = Ae^{j\varphi}(1 - e^{j2\pi\varepsilon})$  and  $a = e^{j\omega}$ . Multiplying both sides of (20) by  $1 - ae^{-j2\pi(k+k_p)/N}$  and rearranging, yields

$$X_L(k) = ae^{-j2\pi(k+k_p)/N} X_L(k) + b + n_L(k) \quad (21)$$

with  $n_L(k) = W_L(k)[1 - ae^{-j2\pi(k+k_p)/N}]$ . The expression (21) can eventually be put in matrix notation as

$$\mathbf{X}_L = \mathbf{P} \begin{bmatrix} a \\ b \end{bmatrix} + \mathbf{n}_L \quad (22)$$

where  $\mathbf{n}_L = [n_L(k); -L_1 \leq k \leq L_2]^T$  is the noise vector and

$$\mathbf{P} = [\mathbf{y}_L \quad \mathbf{u}_L] \quad (23)$$

is an  $(L \times 2)$ -dimensional matrix, whose columns  $\mathbf{y}_L$  and  $\mathbf{u}_L$  have entries  $y_L(k) = e^{-j2\pi(k+k_p)/N} X_L(k)$  and  $u_L(k) = 1$  for  $-L_1 \leq k \leq L_2$ , respectively.

#### B. Estimation algorithm

We use the signal model (22) to get an estimate  $(\hat{a}, \hat{b})$  of the unknown parameters  $(a, b)$ , from which the angular frequency is subsequently retrieved as  $\hat{\omega} = \arg\{\hat{a}\}$ . For this purpose, we observe that the variance of the noise terms  $n_L(k)$  depends on  $a$ . This makes the ML solution difficult to implement, since the maximization of the related likelihood function would require a computationally demanding grid-search over the set spanned by  $(a, b)$ . Such a difficulty is overcome by resorting to the least-squares (LS) concept, which makes no assumption on the noise statistics and can provide a closed-form solution to the estimation of  $(a, b)$ . However, since each DFT sample is characterized by a different SNR value, better results are expected by adopting the WLS approach. This offers the opportunity to emphasize the contributions of those data that are deemed to be more reliable through a suitable design of the weighting coefficients. The latter are denoted by  $\{c(k); -L_1 \leq k \leq L_2\}$  and are collected into an  $L$ -dimensional diagonal matrix  $\mathbf{C} = \text{diag}\{c(k)\}$ . Hence, letting

$$\gamma_c = \sum_{k=-L_1}^{L_2} c(k) \quad (24)$$

we can state the following theorem.

*Theorem 2:* The WLS estimator of  $(a, b)$  based on the model (22) is given by

$$\hat{\omega} = \arg \left\{ \begin{aligned} & \sum_{k=-L_1}^{L_2} c(k) X_L^*(k) \\ & \times \left[ \gamma_c X_L(k) - \sum_{n=-L_1}^{L_2} c(n) X_L(n) \right] e^{j2\pi(k+k_p)/N} \end{aligned} \right\}. \quad (25)$$

*Proof:* Applying the WLS estimation principle to the signal model (22), yields [26]

$$\begin{bmatrix} \hat{a} \\ \hat{b} \end{bmatrix} = (\mathbf{P}^H \mathbf{C} \mathbf{P})^{-1} \mathbf{P}^H \mathbf{C} \mathbf{X}_L. \quad (26)$$

Then, bearing in mind the structure of  $\mathbf{P}$  shown in (23), we can reformulate (26) as

$$\begin{bmatrix} \hat{a} \\ \hat{b} \end{bmatrix} = \frac{1}{\Delta} \begin{bmatrix} \gamma_c & -\mathbf{y}_L^H \mathbf{C} \mathbf{u}_L \\ -\mathbf{u}_L^H \mathbf{C} \mathbf{y}_L & \mathbf{y}_L^H \mathbf{C} \mathbf{y}_L \end{bmatrix} \begin{bmatrix} \mathbf{y}_L^H \mathbf{C} \mathbf{X}_L \\ \mathbf{u}_L^H \mathbf{C} \mathbf{X}_L \end{bmatrix} \quad (27)$$

with

$$\Delta = \gamma_c (\mathbf{y}_L^H \mathbf{C} \mathbf{y}_L) - |\mathbf{u}_L^H \mathbf{C} \mathbf{y}_L|^2. \quad (28)$$

The angular frequency is eventually estimated as  $\hat{\omega} = \arg\{\hat{a}\}$ . This produces

$$\hat{\omega} = \arg\{\gamma_c \mathbf{y}_L^H \mathbf{C} \mathbf{X}_L - \mathbf{y}_L^H \mathbf{C} \mathbf{u}_L \mathbf{u}_L^H \mathbf{C} \mathbf{X}_L\} \quad (29)$$

which is equivalent to (25), thereby concluding the proof of the theorem.

From this point onwards, we call (25) the WLS estimator (WLSE) of  $\omega$ . The peculiar case in which the weighting coefficients are all equal is referred to as the LS estimator (LSE). It is worth noting that for  $L = 2$  the LSE reduces to

$$\hat{\omega} = \arg \left\{ \frac{X_L(0) - X_L(\pm 1)}{X_L(0) - X_L(\pm 1)e^{\mp j2\pi(1+k_p)/N}} \right\} \quad (30)$$

and is mathematically equivalent to the DFT interpolator proposed by Bertocco *et al.* in [7]. Furthermore, when all the DFT samples are involved in the estimation process (i.e.,  $L = N$ ), after lengthy computations the LSE can be reformulated in the time-domain as

$$\hat{\omega} = \arg \left\{ \sum_{n=1}^{N-1} x(n)x^*(n-1) \right\} \quad (31)$$

and corresponds to the linear prediction estimator analyzed by Lank *et al.* in [27]. Its variance is given by

$$\text{var}\{\hat{\omega}\} = \frac{(\text{SNR})^{-1}}{(N-1)^2} \quad (32)$$

and the loss with respect to the CCRB is

$$\frac{\text{var}\{\hat{\omega}\}}{\text{CCRB}} = \frac{N(N+1)}{6(N-1)}. \quad (33)$$

For large data records, the ratio (33) approaches the asymptotic value  $N/6$  and the related loss can be substantial. This suggests how a judicious design of the weights  $\{c(k)\}$  can let WLSE to perform much better than LSE.

### C. Theoretical analysis of WLSE

In order to identify the weighting coefficients that optimize the performance of WLSE, it is important to theoretically assess their impact on the estimation accuracy. Although the analysis can be conducted with any value of  $L \geq 2$ , in the foregoing discussion we assume that  $L$  is odd and let  $L_2 = L_1 = (L-1)/2$ . Such a situation leads to a somewhat simplified mathematical notation and, more importantly, allows to select the  $L$  DFT samples from (7) without any prior knowledge of the FFO polarity. Since the entries of the observation vector  $\mathbf{X}_L = \{X(k_p+k); -L_1 \leq k \leq L_1\}$  are symmetrically placed around the DFT peak  $X(k_p)$ , it is reasonable to use weighting coefficients  $\{c(k); -L_1 \leq k \leq L_1\}$  with a symmetric shape around  $k = 0$ . This amounts to putting  $c(-k) = c(k)$  for  $k = 1, 2, \dots, L_1$ , while  $c(0)$  can be arbitrarily set to unity since the estimate  $\hat{\omega}$  in (25) is not affected if the weights are multiplied by a common normalization coefficient. It follows that only the weighting vector  $\mathbf{c} = [c(1), c(2), \dots, c(L_1)]^T$  is needed for the full design of WLSE.

The accuracy of  $\hat{\omega}$  is assessed in terms of its normalized mean square error (MSE), which is a measure of the loss incurred with respect to the CCRB. Such an indicator depends on  $(\mathbf{c}, L, \varepsilon)$  and is expressed by

$$\rho_{WLSE}(\mathbf{c}, L, \varepsilon) = \frac{\text{E}\{(\hat{\omega} - \omega)^2\}}{\text{CCRB}} \quad (34)$$

with the dependence on  $N$  still being omitted for simplicity. Theoretical analysis conducted in Appendix B leads to the following theorem.

*Theorem 3:* In the high SNR region, WLSE is unbiased and its normalized MSE is found to be

$$\rho_{WLSE}(\mathbf{c}, L, \varepsilon) = \frac{N(N^2-1)}{6\Gamma^2(\xi)} \times \left\{ \sum_{n=1}^{N-1} |\gamma(n, \xi)|^2 - \Re \sum_{n=1}^{N-2} \gamma(n, \xi) \gamma^*(n+1, \xi) \right\} \quad (35)$$

where  $\xi = 2\pi\varepsilon/N$ , while  $\Gamma(\xi)$  and  $\{\gamma(n, \xi); 1 \leq n \leq N-1\}$  are given by

$$\Gamma(\xi) = \sum_{n_1=1}^{N-1} \sum_{n_2=1}^{N-1} e^{j\xi(n_1-n_2)} G_L(n_1, n_2) \quad (36)$$

and

$$\gamma(n, \xi) = \sum_{\ell=1}^{N-1} e^{j\xi(n-\ell)} G_L(n, \ell). \quad (37)$$

The quantities  $G_L(m_1, m_2)$  depend on  $\mathbf{c}$  and are expressed by  $G_L(m_1, m_2) = \gamma_c F_L(m_1 - m_2) - F_L(m_1)F_L(m_2)$ , with

$$F_L(n) = 1 + \sum_{k=1}^{L_1} c(k) \cos(2\pi kn/N). \quad (38)$$

*Proof:* see Appendix B.

### D. Design of the weighting coefficients

At first sight, the minimization of  $\rho_{WLSE}(\mathbf{c}, L, \varepsilon)$  with respect to  $\mathbf{c}$  may appear a good criterion for the design of the WLSE weights. This approach, however, is not useful in practice. The reason is that it would generate a different set of weights for each value of  $\varepsilon$ , thereby optimizing the system performance only for a specific value of the FFO. Since we are interested in a solution that can operate effectively over the entire FFO uncertainty range, the optimization process should be based on an integral performance indicator rather than on a point-wise design criterion. Observing that  $\text{var}\{\hat{\omega}\} \geq \text{CRB}(L, \varepsilon)$  for any unbiased estimator, the normalized CRB defined in (14) represents a lower bound for  $\rho_{WLSE}(\mathbf{c}, L, \varepsilon)$ . Hence, a reasonable approach for the design of  $\mathbf{c}$  is to look for the minimum of the  $p$ -norm distance between  $\rho_{WLSE}(\mathbf{c}, L, \varepsilon)$  and  $\text{NCRB}(L, \varepsilon)$  over the full range  $|\varepsilon| \leq 0.5$ . This results into the following optimization problem

$$\mathbf{c}_{opt} = \arg \min_{\mathbf{c}} \left\{ \int_{-1/2}^{1/2} [\rho_{WLSE}(\mathbf{c}, L, \varepsilon) - \text{NCRB}(L, \varepsilon)]^p d\varepsilon \right\} \quad (39)$$

where popular choices of  $p$  are 1, 2 or infinity. Unfortunately, we were not able to find any explicit expression for  $\mathbf{c}_{opt}$  in (39). Hence, the optimal weights are found through an exhaustive search over the set  $\Omega = \{\mathbf{c} \in \mathbb{R}^{L_1} : 0 \leq c(k) \leq 1 \text{ for } 1 \leq k \leq L_1\}$ . The results obtained with  $L = 3, 5, 7$  using the 2-norm distance are reported in Table I.

As is seen, the optimum weighting coefficients rapidly decay as  $L_1$  increases. For example, we have  $c_{opt}(L_1) = 0.0567$  when  $L = 7$ , thereby revealing that there is little to gain by using values of  $L$  greater than 7. An intuitive explanation

TABLE I  
OPTIMAL WEIGHTING COEFFICIENTS FOR VARIOUS VALUES OF  $L_1$ .

$L$	$\mathbf{c} = [c(1), c(2), \dots, c(L_1)]^T$
3	$\mathbf{c} = [0.6969]$
5	$\mathbf{c} = [0.6338, 0.1347]^T$
7	$\mathbf{c} = [0.6138, 0.1300, 0.0567]^T$

of such a behaviour is that most of the energy of the DFT of a cisoid is concentrated in the peak sample and its two neighbours, while less than 15% of the total energy is collected in the remaining DFT samples [9].

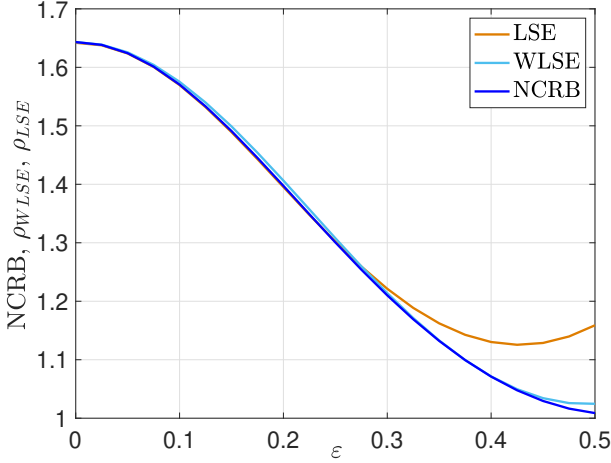


Fig. 3.  $\text{NCRB}(L, \varepsilon)$ ,  $\rho_{\text{WLSE}}(\mathbf{c}_{\text{opt}}, L, \varepsilon)$  and  $\rho_{\text{LSE}}(L, \varepsilon)$  vs.  $\varepsilon \in [0, 0.5]$  with  $L = 3$  and  $N = 64$ .

Fig. 3 illustrates  $\text{NCRB}(L, \varepsilon)$  and  $\rho_{\text{WLSE}}(\mathbf{c}_{\text{opt}}, L, \varepsilon)$  as a function of  $\varepsilon \in [0, 0.5]$  for  $L = 3$ . For comparison, we also report the normalized MSE of LSE, say  $\rho_{\text{LSE}}(L, \varepsilon)$ , which is obtained from  $\rho_{\text{WLSE}}(\mathbf{c}, L, \varepsilon)$  letting  $c(k) = 1$  for  $1 \leq k \leq L_1$ . It is worth noting how a good selection of the weighting coefficients allows the WLSE to perform very close to the normalized bound at any FFO value. In contrast, the LSE attains the bound only for  $|\varepsilon| \leq 0.3$ , with a significant discrepancy occurring around  $\varepsilon = 0.5$ . Fig. 4 shows the same results obtained with  $L = 5$ . As is seen, the WLSE curve is still close to the bound. Compared with the case  $L = 3$ , however, the MSE is approximately reduced by a factor 1.25 (corresponding to nearly 1 dB) at small FFO values, while it remains more or less the same in the proximity of  $\varepsilon = 0.5$ . Results obtained with  $L = 7$  confirm this trend, thereby revealing how parameter  $L$  can be exploited to improve the estimation accuracy. As for LSE, it exhibits a significant loss with respect to the bound and performs even worse than with  $L = 3$ . This suggests how a good design of the weights  $\mathbf{c}$  is fundamental to achieve satisfactory performance.

Having established that WLSE is able to approach the bound to the accuracy of any direct DFT interpolator, the question arises as to whether some strong motivation exists for its use, given that iterative estimators, such as those reported in [25], can perform close to the CCRB. One possible answer comes from the complexity analysis presented below.

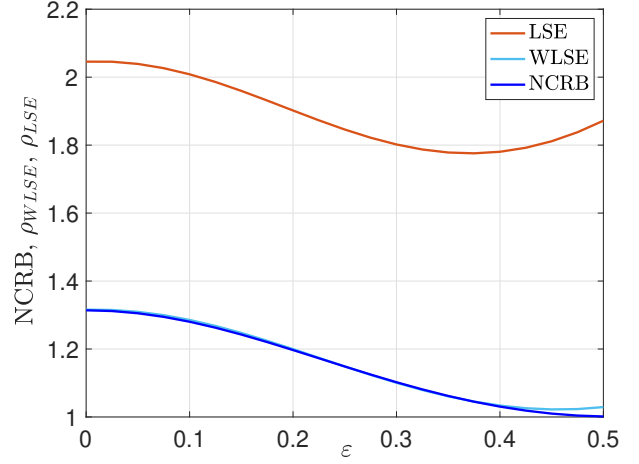


Fig. 4.  $\text{NCRB}(L, \varepsilon)$ ,  $\rho_{\text{WLSE}}(\mathbf{c}_{\text{opt}}, L, \varepsilon)$  and  $\rho_{\text{LSE}}(L, \varepsilon)$  vs.  $\varepsilon \in [0, 0.5]$  with  $L = 5$  and  $N = 64$ .

TABLE II  
COMPUTATIONAL REQUIREMENTS OF DIFFERENT ESTIMATORS

Estimators	Number of flops	Case study, $N = 64$
WLSE	$5N \log_2 N + 20L - 10$	$1910 + 20L$
QE	$5N \log_2 N + 17$	1937
ME ( $L = 3$ )	$5N \log_2 N + 21$	1941
ME ( $L = 5$ )	$5N \log_2 N + 28$	1948
CE	$5N \log_2 N + 14$	1934
QSE	$5N \log_2 N + 48N + 33$	5025
AHSE	$5N \log_2 N + 32N + 22$	3990

### E. Complexity analysis

In assessing the processing requirement of WLSE, we observe that the  $N$ -point DFT employed in the coarse search needs  $(N/2) \log_2 N$  complex products and  $N \log_2 N$  complex additions. Since a complex product amounts to four real products plus two real additions, while a complex additions is equivalent to two real additions, a total of  $(5N) \log_2 N$  floating point operations (flops) are required for the initial DFT. Then, assuming that the weights  $\mathbf{c}$  have been precomputed, additional  $20L - 10$  flops are eventually needed to compute  $\hat{\omega}$  from (25).

The overall complexity of WLSE is summarized in the first row of Tab. II for a general value of  $N$  (first column) and for  $N = 64$  (second column). For comparison, we also report the complexity of other non-iterative DFT interpolation methods, including the bias-removed version of the estimators proposed by Quinn [8], Macleod [9] and Candan [12]. For notational conciseness, we denote these schemes as QE, ME and CE, respectively. While QE and CE can only use the DFT peak and its two neighbours ( $L = 3$ ), ME can be implemented with either  $L = 3$  or  $L = 5$ . The results of Tab. II indicate that direct interpolation methods entail negligible additional cost with respect to the initial DFT operation. This may not be true with iterative schemes, especially for relatively small values of  $N$ . Indeed, computing two extra DFT coefficients at each new iteration requires  $2N$  complex products and  $2(N - 1)$  complex additions, for a total of  $16N - 4$  flops. In the last two rows of Tab. II we report the overall complexity of two recently proposed iterative interpolators, i.e., the  $q$ -shift

estimator (QSE) and the hybrid A&M and  $q$ -shift estimator (HAQSE) presented in [25]. The former scheme requires three iterations to achieve convergence, while the latter converges after two iterations. In any case, they are much more computationally demanding than direct interpolation alternatives. In particular, for  $N = 64$  we see that computing the extra DFT coefficients needs more flops than the initial  $N$ -point DFT. A further disadvantage of iterative schemes is that they must re-elaborate the entire time series  $\{x(n)\}$  at each new iteration to obtain the extra DFT coefficients. This operation cannot be performed in real-time, which makes them unsuitable for those applications where frequency estimation must be accomplished fast and efficiently, in compliance with the time constraints of the system. In contrast, WLSE can be put in a condition to perform similarly to iterative schemes without the need for computing any additional DFT coefficient. In fact, it is enough to increase  $L$  so as to achieve the desired accuracy at the price of a marginal increment of the processing load, which still remains negligible with respect to the cost of the initial DFT.

It is worth recalling that WLSE is only suited for single-tone frequency recovery, while in some situations the received signal can be plagued by harmonic interference. In these applications, using a relatively large value of  $L$  might be a bad choice, as interference is more likely to be included in the estimation process. However, since in this work the number of interpolated DFT coefficients is limited to a few units, the WLSE explores a narrow bandwidth around the DFT peak, where the probability of finding harmonic interference is expected to be low.

## V. NUMERICAL RESULTS

Computer simulations have been run to assess the performance of WLSE and to check the analytical results reported in Sect. IV.C. In all the presented experiments, the number of data samples is  $N = 64$  while the IFO is set to  $k_p = 10$ . Comparisons are made between WLSE and other non-iterative DFT interpolation methods, such as QE, ME and CE. We also consider the FFO recovery algorithm suggested by Orguner (OE) in [10], although we limit its application to the first iteration stage. The reason is that in this study we are only interested to the class of direct DFT interpolators, which operate in a non-iterative fashion.

Fig. 5 illustrates the MSE of the frequency estimate  $\hat{\omega}/(2\pi)$  as a function of the SNR. The number of interpolated DFT coefficients is  $L = 3$  and the FFO is uniformly distributed over the interval  $[-0.5, 0.5]$ . The CCRB given in (4), divided by  $4\pi^2$ , is also shown as a benchmark. As it is seen, when the SNR decreases all the curves show an abrupt increase, which reflects the insurgence of outliers. The SNR at which the increase begins establishes the estimator threshold, which occurs at nearly 0 dB. When operating above the threshold, WLSE and ME have the best performance and their accuracy is approximately 1.5 dB far from the CCRB. The loss increases to 2.5 dB when using QE and becomes nearly 4 dB with CE and OE. Other simulations (not shown) indicate that all the considered schemes provide unbiased estimates over the full range  $[-0.5, 0.5]$ .

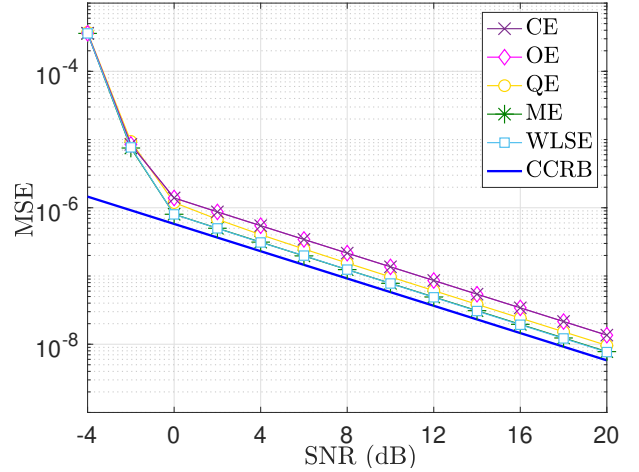


Fig. 5. MSE of the frequency estimate  $\omega/2\pi$  vs. SNR with  $L = 3$  and  $N = 64$ .

Fig. 6 plots the normalized MSE defined in (34) versus  $\varepsilon \in [0, 0.5]$  for WLSE (with optimized weighting coefficients), LSE, ME and OE. In this experiment we have  $L = 3$  and the SNR is fixed to 20 dB. It is worth noting how the proposed WLSE is close to the normalized CRB given in (15) over the entire range of FFO values, while LSE exhibits a certain performance degradation for  $\varepsilon > 0.3$ . The ME is characterized by a good accuracy, with only a marginal loss with respect to WLSE in the region  $\varepsilon \in [0.1, 0.4]$ . As for OE, its normalized MSE deviates substantially from the bound and the loss increases with  $\varepsilon$ . Such a behaviour is also documented in [10], where an SNR gap of nearly 5 dB with respect to the bound was found at the end of the first iteration for FFO values close to  $\pm 0.5$ .

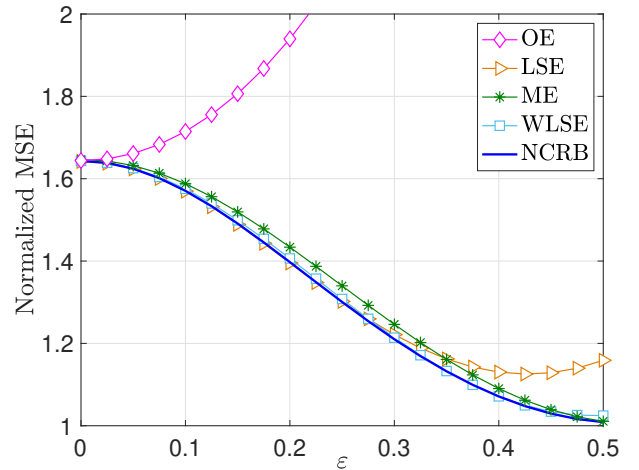


Fig. 6. Normalized MSE vs.  $\varepsilon \in [0, 0.5]$  with  $L = 3$ ,  $N = 64$  and SNR = 20 dB.

The MSE of the frequency estimates obtained through interpolation of  $L = 5$  DFT coefficients is shown in Fig. 7 as a function of the SNR. In this figure, WLSE is compared with ME and OE, which are the only non-iterative schemes available in the literature that can operate with more than



$L = 3$  DFT samples. The trend is similar to what is reported in Fig. 5. In particular, the best accuracy is achieved by WLSE (with optimized weights) and ME, for which the gap with respect to the CCRB is now reduced to only 1 dB. In contrast, OE exhibits a significant loss compared to the bound. It is worth observing that when  $L = 5$  the ME presented in [9] is based on a heuristic formula that is not supported by any theoretical argument. Hence, it is important to check whether the resulting FFO estimates are biased or not. The result of this study is illustrated in Fig. 8, where the bias of the investigated schemes is shown as a function of  $\varepsilon$  in the absence of noise. As it is seen, ME provides FFO estimates with a bias that can be greater than  $2 \times 10^{-5}$ , while WLSE and OE are found to be unbiased.

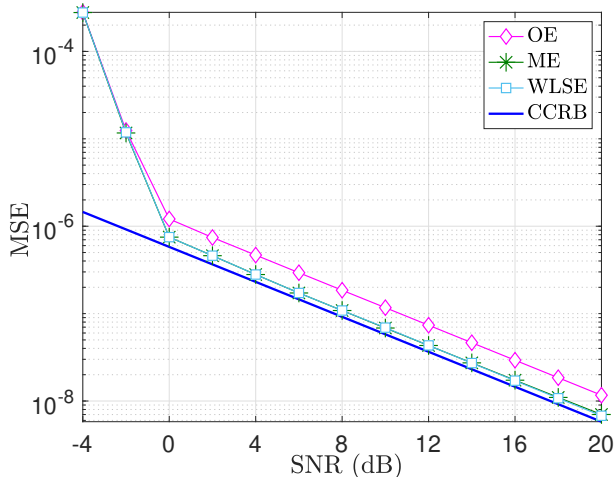


Fig. 7. MSE of the frequency estimate  $\omega/2\pi$  vs. SNR with  $L = 5$  and  $N = 64$ .

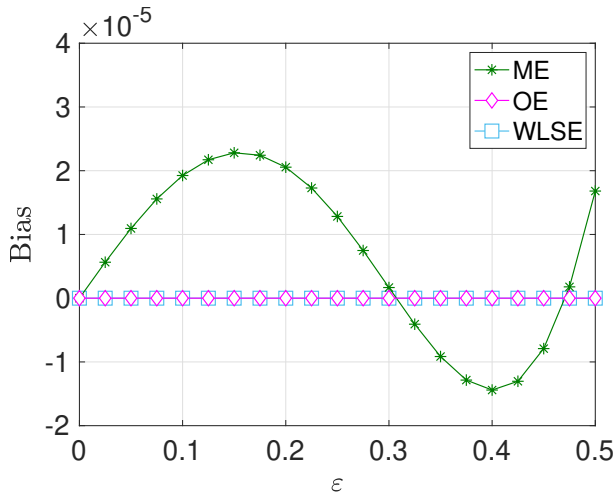


Fig. 8. Bias of the frequency estimate  $\omega/2\pi$  vs.  $\varepsilon \in [0, 0.5]$  in absence of noise with  $L = 5$  and  $N = 64$ .

Fig. 9 illustrates the normalized MSE for the investigated DFT interpolators as a function of  $\varepsilon$  when  $L = 5$  and SNR = 20 dB. Similarly to the  $L = 3$  case, the best accuracy is obtained with WLSE, which closely follows the normalized

CRB curve at any FFO value, with only a marginal discrepancy in the proximity of  $\varepsilon = 0.5$ . The ME still exhibits satisfactory performance, even though the loss with respect to the bound in the region  $\varepsilon \in [0.1, 0.4]$  is larger than in Fig. 6. As expected, the accuracy of OE deteriorates as  $\varepsilon$  approaches the boundary values  $\pm 0.5$ , while LSE is far from the bound over the full FFO interval.

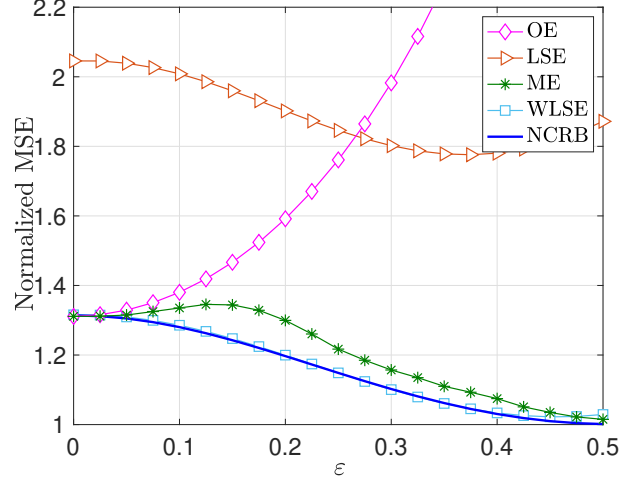


Fig. 9. Normalized MSE vs.  $\varepsilon \in [0, 0.5]$  with  $L = 5$ ,  $N = 64$  and SNR = 20 dB.

## VI. CONCLUSIONS

We have discussed the problem of fine frequency recovery for a single discrete-time spectral line through DFT interpolation methods. The focus was on fast non-iterative schemes that avoid the need for computing extra DFT coefficients in addition to those available from the initial coarse search stage. A first contribution of this work is the analytical formulation of the CRB for this class of methods, which only exploit a reduced set of DFT coefficients to complete the fine estimation process. The resulting expression has general applicability and can be used with any value of the system parameters. It extends some known results that were previously obtained in a few specific scenarios under the assumption of large data records. The second contribution is the derivation of a novel DFT interpolation scheme (WLSE) based on the weighted least-squares approach. Theoretical analysis indicates that an appropriate design of the weighting coefficients leads to an estimation accuracy close to the relevant CRB at any value of the residual frequency error. This suggests that there is very little room for further improvement of the estimation accuracy through direct DFT interpolation techniques. Numerical simulations have been used to corroborate such a conjecture. In particular, it was found that WLSE has the best accuracy among existing non-iterative methods, which makes it the preferred scheme for fast real-time frequency recovery. In contrast to most available methods, which only use the DFT peak and its two neighbours, WLSE has the capability of interpolating an arbitrary number  $L$  of DFT coefficients. Assuming that no harmonic interference is present in the explored signal bandwidth, this offers the opportunity, through a judicious design of  $L$ , to approach the

performance of iterative DFT interpolators, with a significant reduction of the computational load and processing time.

## VII. ACKNOWLEDGMENT

The authors are grateful to Tommaso Morelli, who made a preliminary search for the optimal WLSE weights.

## VIII. APPENDIX A

In this Appendix, we compute the CRB for the estimation of the angular frequency  $\omega$  using the observation vector  $\mathbf{X}_L$ . The presence of the nuisance parameters  $\{C_R, C_I\}$  requires evaluation of the Fisher information matrix (FIM) for the set  $\zeta = \{C_R, C_I, \omega\}$ . For this purpose, we rewrite (8) in vector notation as

$$\mathbf{X}_L = \mathbf{S}_L + \mathbf{W}_L \quad (40)$$

where  $\mathbf{S}_L = \{S_L(k); -L_1 \leq k \leq L_2\}$  collects the quantities reported in (9), while  $\mathbf{W}_L = \{W_L(k); -L_1 \leq k \leq L_2\}$  is a Gaussian vector with zero mean and covariance matrix  $\mathbf{C}_W = \sigma_W^2 \mathbf{I}_L$ . The entries of the FIM for a complex-valued vector  $\mathbf{S}_L$  embedded in white Gaussian noise are evaluated in Appendix 15C of [26] and are given by

$$[\mathbf{F}]_{i,j} = 2\Re \left\{ \frac{\partial \mathbf{S}_L^H}{\partial \zeta_i} \mathbf{C}_W^{-1} \frac{\partial \mathbf{S}_L}{\partial \zeta_j} \right\} \quad 1 \leq i, j \leq 3 \quad (41)$$

where we have used the notation  $\zeta_1 = C_R$ ,  $\zeta_2 = C_I$  and  $\zeta_3 = \omega$ . Then, expanding the vector multiplication in the right-hand-side of (41), produces

$$[\mathbf{F}]_{i,j} = \frac{2}{\sigma_W^2} \sum_{k=-L_1}^{L_2} \Re \left\{ \frac{\partial S_L^*(k)}{\partial \zeta_i} \cdot \frac{\partial S_L(k)}{\partial \zeta_j} \right\} \quad 1 \leq i, j \leq 3. \quad (42)$$

The derivatives of  $S_L(k)$  with respect to the unknown parameters are easily computed from (9) as

$$\frac{\partial S_L(k)}{\partial C_R} = N\alpha(k) \quad (43)$$

$$\frac{\partial S_L(k)}{\partial C_I} = jN\alpha(k) \quad (44)$$

$$\frac{\partial S_L(k)}{\partial \omega} = jNAe^{j\varphi}\beta(k) \quad (45)$$

where  $\alpha(k)$  and  $\beta(k)$  depend on the FFO  $\varepsilon$  and are expressed by

$$\alpha(k) = \frac{1}{N} \sum_{n=0}^{N-1} e^{-j2\pi n(k-\varepsilon)/N} \quad (46)$$

$$\beta(k) = \frac{1}{N} \sum_{n=0}^{N-1} ne^{-j2\pi n(k-\varepsilon)/N}. \quad (47)$$

Substituting these results into (42) yields the FIM

$$\mathbf{F} = \frac{2N}{\sigma^2} \begin{bmatrix} \|\boldsymbol{\alpha}\|^2 & 0 & \mu_I \\ 0 & \|\boldsymbol{\alpha}\|^2 & \mu_R \\ \mu_I & \mu_R & A^2 \|\boldsymbol{\beta}\|^2 \end{bmatrix} \quad (48)$$

where  $\mu = \mu_R + j\mu_I$  is given by

$$\mu = Ae^{-j\varphi}(\boldsymbol{\beta}^H \boldsymbol{\alpha}) \quad (49)$$

and we have defined the  $L$ -dimensional vectors  $\boldsymbol{\alpha} = \{\alpha(k); -L_1 \leq k \leq L_2\}$  and  $\boldsymbol{\beta} = \{\beta(k); -L_1 \leq k \leq L_2\}$ . Letting  $\mathbf{F}^{-1}$  be the inverse of  $\mathbf{F}$ , the CRB for the estimation of  $\omega$  is  $[\mathbf{F}^{-1}]_{3,3}$ . This is computed from (48) through a standard matrix inversion operation, yielding

$$\text{CRB}(L, \varepsilon) = \frac{\sigma^2}{2NA^2} \cdot \frac{\|\boldsymbol{\alpha}\|^2}{\|\boldsymbol{\alpha}\|^2 \|\boldsymbol{\beta}\|^2 - |\boldsymbol{\beta}^H \boldsymbol{\alpha}|^2} \quad (50)$$

where the notation  $\text{CRB}(L, \varepsilon)$  is used to explicitly indicate the dependence of the bound on the parameters  $L$  and  $\varepsilon$ . A simplified expression of the CRB is obtained when  $\varepsilon = 0$ . In such a case, from (46) and (47) it follows that  $\alpha(k)$  is one only for  $k = 0$  and it is zero otherwise, while

$$\beta(k) = \begin{cases} 1/(e^{-j2\pi k/N} - 1) & \text{if } k \neq 0 \\ (N-1)/2 & \text{if } k = 0. \end{cases} \quad (51)$$

Consequently, we have  $\|\boldsymbol{\alpha}\|^2 = 1$ ,  $\boldsymbol{\beta}^H \boldsymbol{\alpha} = (N-1)/2$  and

$$\|\boldsymbol{\beta}\|^2 = \frac{(N-1)^2}{4} + \sum_{k \in \mathcal{A}} \frac{1}{|e^{-j2\pi k/N} - 1|^2} \quad (52)$$

where  $\mathcal{A}$  is the set of integers  $k$  such that  $-L_1 \leq k \leq L_2$  and  $k \neq 0$ . Substituting these results into (50), produces

$$\text{CRB}(L, \varepsilon) = \frac{2\sigma^2}{NA^2 \sum_{k \in \mathcal{A}} \frac{1}{\sin^2(\pi k/N)}}. \quad (53)$$

## IX. APPENDIX B

In this Appendix, we highlight the major steps leading to the theoretical performance of WLSE. We begin by rewriting (25) as

$$\hat{\omega} = \arg \{\gamma_c A_1 - A_2\} \quad (54)$$

where

$$A_1 = \sum_{k=-L_1}^{L_2} c(k) |X_L(k)|^2 e^{j2\pi(k+k_p)/N} \quad (55)$$

and

$$A_2 = \sum_{k=-L_1}^{L_2} c(k) X_L^*(k) e^{j2\pi(k+k_p)/N} \sum_{m=-L_1}^{L_2} c(m) X_L(m). \quad (56)$$

Our first objective is to find a time-domain representation of  $A_1$  and  $A_2$ . For this purpose, we replace the DFT coefficients  $X_L(k)$  in (55) and (56) by

$$X_L(k) = \sum_{n=0}^{N-1} x(n) e^{-j2\pi n(k+k_p)/N}. \quad (57)$$

After standard manipulations, this yields

$$A_1 = \sum_{n_1=0}^{N-1} \sum_{n_2=1}^N x(n_1) x^*(n_2-1) e^{-j\pi K(n_1-n_2)/N} F_L(n_1-n_2) \quad (58)$$

and

$$A_2 = \sum_{n_1=0}^{N-1} \sum_{n_2=1}^N x(n_1) x^*(n_2-1) \times e^{-j\pi K(n_1-n_2)/N} F_L(n_1) F_L(n_2) \quad (59)$$

where  $K = 2k_p + L_2 - L_1$ , while  $F_L(n)$  is a real-valued even function of  $n$  expressed by

$$F_L(n) = \sum_{k=-L_1}^{L_2} c(k) e^{-j\pi(2k-L_2+L_1)n/N} \quad (60)$$

which depends on the selected weights  $\{c(k)\}$ . Substituting (58) and (59) into (54), produces

$$\hat{\omega} = \arg \left\{ \sum_{n_1=0}^{N-1} \sum_{n_2=1}^N x(n_1) x^*(n_2 - 1) \times e^{-j\pi K(n_1 - n_2)/N} G_L(n_1, n_2) \right\} \quad (61)$$

where

$$G_L(n_1, n_2) = \gamma_c F_L(n_1 - n_2) - F_L(n_1) F_L(n_2) \quad (62)$$

is a real-valued function. Finally, observing that  $G_L(0, n_2) = G_L(n_1, N) = 0$ , we can rewrite (61) as

$$\hat{\omega} = \arg \left\{ \sum_{n_1=1}^{N-1} \sum_{n_2=1}^{N-1} x(n_1) x^*(n_2 - 1) \times e^{-j\pi K(n_1 - n_2)/N} G_L(n_1, n_2) \right\} \quad (63)$$

which can be interpreted as the time-domain formulation of WLSE. Such expression is now used to assess the accuracy of  $\hat{\omega}$ . For this purpose, it is convenient to put the time series  $\{x(n)\}$  in the equivalent form

$$x(n) = A e^{j(\omega n + \varphi)} [1 + \mu(n)] \quad n = 0, 1, \dots, N-1 \quad (64)$$

where  $\{\mu(n) = w(n) e^{-j(\omega n + \varphi)} / A\}$  are statistically independent noise terms with zero mean and variance  $\sigma_\mu^2 = \sigma^2 / A^2$ . Then, after substituting (64) into (63), we find

$$\hat{\omega} = \arg \left\{ e^{j\omega} \sum_{n_1=1}^{N-1} \sum_{n_2=1}^{N-1} [1 + \mu(n_1)] \times [1 + \mu^*(n_2 - 1)] e^{j\xi(n_1 - n_2)} G_L(n_1, n_2) \right\} \quad (65)$$

where  $\xi$  is related to the FFO  $\varepsilon$  by the following relationship

$$\xi = \frac{\pi}{N} (2\varepsilon - L_2 + L_1). \quad (66)$$

To simplify the analysis, we assume that the SNR is large enough to make the Noise $\times$ Noise term  $\mu(n_1)\mu^*(n_2 - 1)$  negligible (with high probability) with respect to  $\mu(n_1)$  or  $\mu^*(n_2 - 1)$ . In such a case, the estimate (65) can reasonably be approximated as

$$\hat{\omega} = \arg \left\{ e^{j\omega} \Gamma(\xi) [1 + D(\xi)] \right\} \quad (67)$$

where  $\Gamma(\xi)$  is a real-valued positive quantity given by

$$\Gamma(\xi) = \sum_{n_1=1}^{N-1} \sum_{n_2=1}^{N-1} e^{j\xi(n_1 - n_2)} G_L(n_1, n_2) \quad (68)$$

while  $D(\xi)$  is found to be

$$D(\xi) = \frac{1}{\Gamma(\xi)} \sum_{n=1}^{N-1} [\mu(n)\gamma(n, \xi) + \mu^*(n-1)\gamma^*(n, \xi)] \quad (69)$$

with

$$\gamma(n, \xi) = \sum_{\ell=1}^{N-1} e^{j\xi(n-\ell)} G_L(n, \ell). \quad (70)$$

Observing that  $\Gamma(\xi) \in \mathbb{R}^+$ , we can rewrite (67) as

$$\hat{\omega} = \arg \left\{ e^{j\omega} [1 + D(\xi)] \right\}. \quad (71)$$

Accordingly, since when the SNR is large the real and imaginary components of  $D(\xi)$ , say  $D_R(\xi)$  and  $D_I(\xi)$ , are much less than unity, from (71) we have

$$\hat{\omega} \approx \omega + D_I(\xi) \quad (72)$$

which says that WLSE is unbiased because  $D(\xi)$  is a zero-mean random variable. The estimation variance is given by

$$\text{var}\{\hat{\omega}\} \approx \text{E}\{D_I^2(\xi)\} \quad (73)$$

and can eventually be computed making use of the noise statistics

$$\text{E}\{\mu(n_1)\mu^*(n_2)\} = \begin{cases} \sigma^2/A^2 & \text{if } n_1 = n_2 \\ 0 & \text{otherwise} \end{cases} \quad (74)$$

and  $\text{E}\{\mu(n_1)\mu(n_2)\} = \text{E}\{\mu^*(n_1)\mu^*(n_2)\} = 0$ . After lengthy standard computations, we find

$$\text{var}\{\hat{\omega}\} = \frac{\sigma^2}{A^2 \Gamma^2(\xi)} \times \left\{ \sum_{n=1}^{N-1} |\gamma(n, \xi)|^2 - \Re \sum_{n=1}^{N-2} \gamma(n, \xi) \gamma^*(n+1, \xi) \right\}. \quad (75)$$

## REFERENCES

- [1] M. A. Richards, *Fundamentals of Radar Signal Processing*, New York, NY, USA: McGraw-Hill, 2005.
- [2] Y. Xia, Y. He, K. Wang, W. Pei, Z. Blazic, and D. P. Mandic, "A complex least squares enhanced smart DFT technique for power system frequency estimation", *IEEE Trans. Power Del.*, vol. 32, no. 3, pp. 1270-1278, Jun. 2017.
- [3] D. C. Rife and R. R. Boorstyn, "Single-tone parameter estimation from discrete-time observations", *IEEE Trans. Inf. Theory*, vol. 20, no. 5, pp. 591-598, Sep. 1974.
- [4] P. Voglewede, "Parabola approximation for peak determination", *Global DSP Mag.*, vol. 3, no. 5, pp. 13-17, May 2004.
- [5] V. K. Jain, W. L. Collins, Jr., and D. C. Davis, "High-accuracy analog measurements via interpolated FFT", *IEEE Trans. on Instrum. and Measurement*, vol. IM-28, no. 2, pp. 113-122, Jun. 1979.
- [6] T. Grandke, "Interpolation algorithms for Discrete Fourier Transforms of weighted signals", *IEEE Trans. on Instrum. and Measurement*, vol. IM-32, no. 2, pp. 350-355, Jun. 1983.
- [7] M. Bertocco, C. Offelli, and D. Petri, "Analysis of damped sinusoidal signals via frequency domain interpolation algorithm", *IEEE Instrum. and Measurement Technology Conf.*, pp. 437-440, 18-20 May, 1993.
- [8] B. G. Quinn, "Estimation of frequency, amplitude and phase from the DFT of a time series", *IEEE Trans. on Signal Processing*, vol. 45, no. 3, pp. 814-817, Mar. 1997.
- [9] M. D. Macleod, "Fast nearly ML estimation of the parameters of real or complex single tones or resolved multiple tones", *IEEE Trans. on Signal Processing*, vol. 46, no. 1, pp. 141-148, Jan. 1998.
- [10] U. Orguner and C. Candan, "A fine-resolution frequency estimator using an arbitrary number of DFT coefficients", *Signal Processing*, Elsevier, vol. 105, no. 10, pp. 17-21, Dec. 2014.
- [11] E. Jacobsen and P. Kootsookos, "Fast, accurate frequency estimators", *IEEE Signal Processing Magazine*, vol. 24, no. 3, pp. 123-125, May 2007.
- [12] C. Candan, "A method for fine resolution frequency estimation from three DFT samples", *IEEE Signal Processing Letters*, vol. 18, no. 6, pp. 351-354, Jun. 2011.

- [13] C. Candan, "Analysis and further improvement of fine resolution frequency estimation method from three DFT samples", *IEEE Signal Processing Letters*, vol. 20, no. 9, pp. 913-916, Sept. 2013.
- [14] J.-R. Liao and S. Lo, "Analytical solutions for frequency estimators by interpolation of DFT coefficients", *Signal Processing*, Elsevier, vol. 93, 2014.
- [15] L. Fang, D. Duan, and L. Yang, "A new DFT-based frequency estimator for single-tone complex sinusoidal signals", in *Proc. of MILCOM 2012 - 2012 Military Commun. Conference*, 2012.
- [16] X. Liang, A. Liu, X. Pan, Q. Zhang, and F. Chen, "A new and accurate estimator with analytical expression for frequency estimation", *IEEE Commun. Letters*, vol. 20, no. 1, pp. 105-108, Jan. 2016.
- [17] Y. Chen, A. H. C. Ko, W. S. Tam, C. W. Kok, and H. C. So, "Non-iterative and accurate frequency estimation of a single cisoid using two DFT coefficients", *Digital Signal Processing*, Elsevier, vol. 98, Mar. 2020.
- [18] Y. V. Zakharov and T. C. Tozer, "Frequency estimator with dichotomous search of periodogram peak", *Electronics Letters*, vol. 35, no. 19, pp. 1608-1609, Sept. 1999.
- [19] T. J. Abatzoglou, "A fast maximum likelihood algorithm for frequency estimation of a sinuosid based on Newton's method", *IEEE Trans. Acoustic, Speech, Signal Processing*, vol. ASSP-33, pp. 77-89, Dec. 1985.
- [20] E. Aboutanios and B. Mulgrew, "Iterative frequency estimation by interpolation of Fourier coefficients", *IEEE Trans. on Signal Processing*, vol. 53, no. 4, pp. 1237-1242, Apr. 2005.
- [21] Y. Liu, Z. Nie, Z. Zhao, and Q. H. Liu, "Generalization of iterative Fourier interpolation algorithms for single frequency estimation", *Digital Signal Processing*, vol. 21, no. 1, pp. 141-149, Jan 2011.
- [22] C. Gong, D. Guo, B. Zhang, and A. Liu, "Improved frequency estimation by interpolated DFT method", *2012 Int. Workshop on Information and Electronics Engineering (IWIEE)*, pp. 4112-4116, Elsevier, 2012.
- [23] S. F. Minhas and P. Gaydecki, "A non-iterative approach to frequency estimation of a complex exponential in noise by interpolation of Fourier coefficients", *IEEE 18th Int. Conf. on Digital Signal Processing (DSP)*, 2013.
- [24] L. Fan and G. Qi, "Frequency estimator of a sinusoid based on interpolation of three DFT spectral lines", *Signal Processing*, Elsevier, vol. 144, pp. 52-60, Mar. 2018.
- [25] A. Serbes, "Fast and efficient sinusoidal frequency estimation by using the DFT coefficients", *IEEE Trans. on Communications*, vol. 67, no. 3, pp. 2333-2342, Mar. 2019.
- [26] S. M. Kay, *Fundamentals of Statistical Signal Processing: Estimation Theory*, Prentice Hall, Englewood Cliffs, New Jersey, 1993.
- [27] G. W. Lank, I. S. Reed, G. E. Pollon, "A semicoherent detection and doppler estimation statistic", *IEEE Trans. on Aerospace and Electronic Systems*, vol. AES-9, no. 2, pp. 151-165, Mar. 1973.